

## LED Goniometry System

L. Svilainis, V. Dumbrava

Department of Signal Processing, Kaunas University of Technology,  
Studentu str. 50, LT-51368 Kaunas, Lithuania, tel.: +370 37 300532, e-mail: svilnis@ktu.lt

### Introduction

More than thirty years have passed since Light Emitting Diode (LED) was developed and twenty years since it began to be utilized for displaying information. The LED displays are used in the road and railway signage facilities [1], banks, stock exchange, airports [2], events and advertising [3].

LED parameters define the final image quality. The LED can be specified by such parameters as luminous intensity, luminous flux, radiant intensity, radiant flux, peak and dominant wavelength, chromaticity coordinates and efficiency [4-6]. The LED directivity parameters are important in video screen applications. They define both the image purity and the screen image quality at various viewing angles. The directivity diagram, usually called far-field pattern (FFP) can be used to calculate the numerical parameters: full width half max and peak emission angles.

The system discussed in this paper is dedicated for the LED directivity diagram measurement. The accuracy issues and prototype system have already been discussed in [7]. We will be concentrating on system design approaches and system capabilities investigation.

### LED directivity parameters

The LED far-field pattern measurement is performed by measuring the intensity  $I_v$  distribution as a observation angle  $\theta$ . The diagram [7] explaining the LED FFP measurement procedure is presented in Fig. 1.

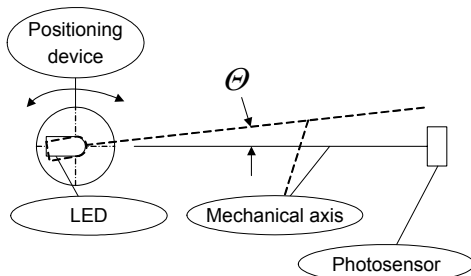


Fig. 1. For LED goniometry explanation

The obtained  $I_v(\theta)$  is usually normalized by peak emission value and can be plotted in Cartesian coordinate system (Fig.2) or polar coordinate system (refer to Fig.3).

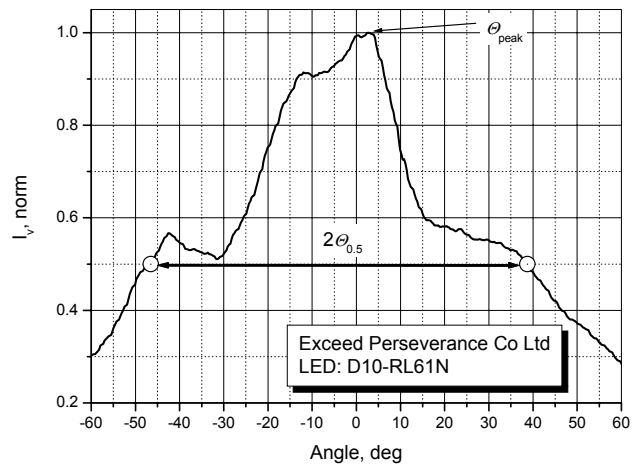


Fig. 2. Measured D10 LED FFP in Cartesian system

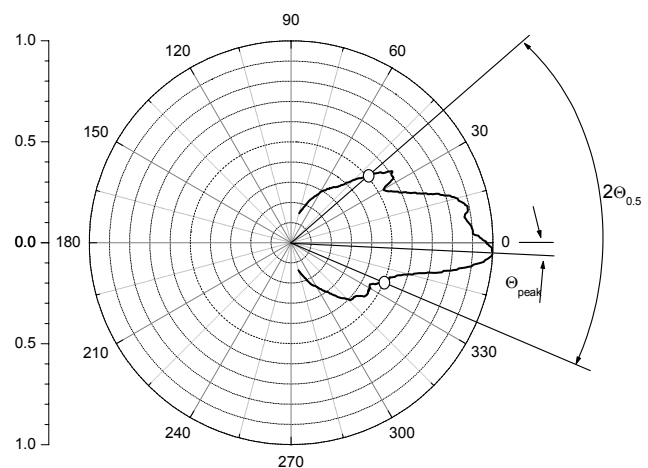


Fig. 3. Measured LED D10 FFP in polar system

Now numerical parameters can be obtained from the FFP - the peak emission direction  $\theta_{peak}$  and half power beam angle  $2\theta_{0.5}$  where the source's relative intensity is

dropping to the half of the peak emission. Refer to Fig. 4. for  $\theta_{\text{peak}}$  and  $2\theta_{0.5}$  physical meaning explanation.

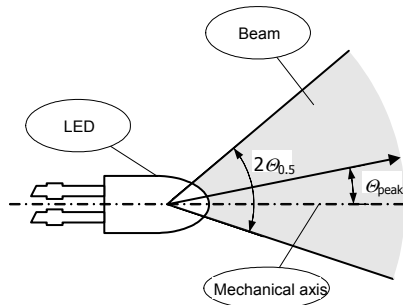


Fig. 4. For  $\theta_{\text{peak}}$  and  $2\theta_{0.5}$  explanation

Finally, having a measured FFP, screen FFP can be calculated. The screen FFP [8] differs from individual LED FFP – usually it's wider. Turn to Fig. 5 for explanation.

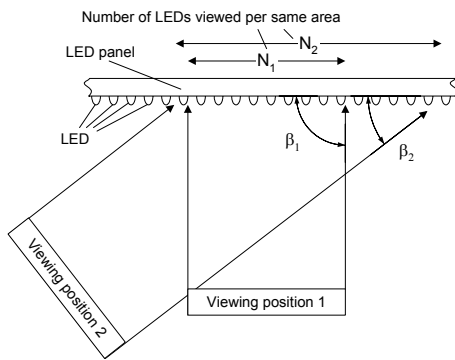


Fig. 5. For screen FFP explanation

When viewing a LED video display, the human eye is gathering light not from a single LED, but from a given area of the display. As the spectator moves off-center, observing the screen at sharper angle, this area actually increases (refer Fig. 5). This effect will modify the screen light response. Using the geometry indicated in Fig. 5 screen FFP  $I_{SC}(\beta)$  can be calculated

$$I_{SC}(\beta) = \frac{I_V(\pi - \beta)}{\sin(\beta)} \quad (1)$$

It could be easily derived from Fig.4 and Fig.5 that

$$\Theta = \pi - \beta \quad (2)$$

Therefore screen FFP using angles of LED FFP:

$$I_{SC}(\Theta) = \frac{I_V(\Theta)}{\sin(\pi - \Theta)} \quad (3)$$

The measured LED FFP, indicated in Fig.2 and Fig.3 has been converted using equation (3) into screen FFP. The resulting FFP is presented in Fig.6.

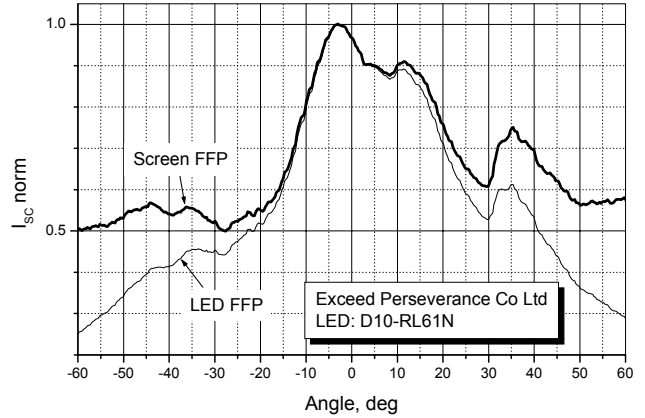


Fig. 6. Calculated D10 screen FFP in Cartesian system

One can note in Fig. 6 that the screen response FFP is wider than individual LED. The level of this viewing angle broadening will depend on the shape of the LED FFP. Of course, it would be logical to use averaged LED FFP from several measurements in order to construct the screen FFP, since not the individual but statistical LED response will form the screen FFP.

### The measurement system

In order to estimate the possibilities of photo goniometry, a prototype system has been developed. Refer to publication [7] for detailed description and feasibility study results. Basing the analysis done in feasibility study using the prototype system, new system has been developed (refer Fig. 6). From the explanation of LED goniometry, presented in Fig. 1, system must contain the positioning device and the radiometry sensor.

The step motor has been chosen as the angular

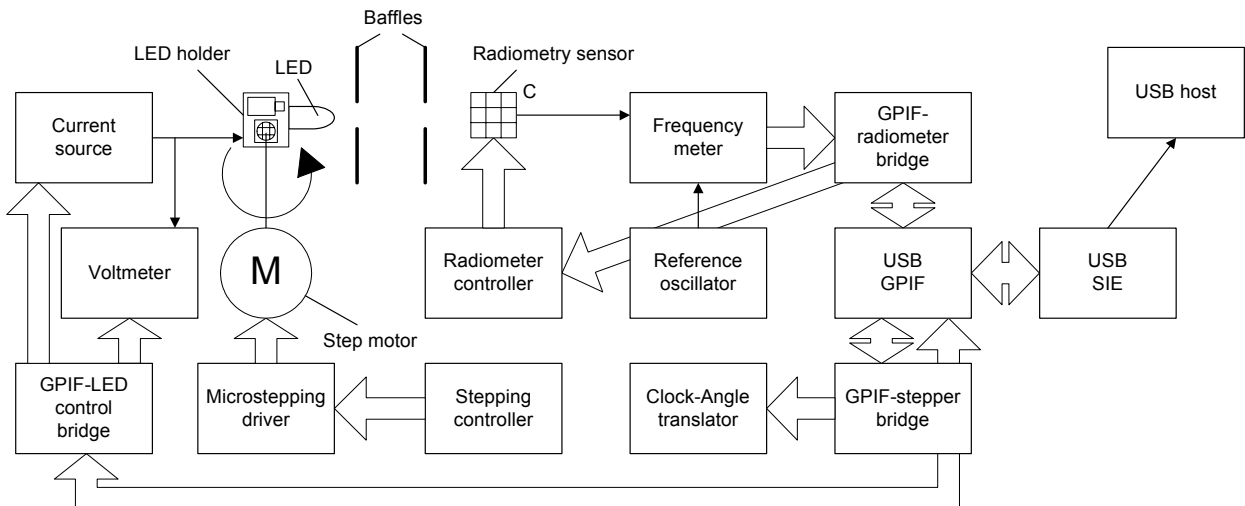


Fig. 7. Goniometry system structure

positioning device. The motor is a torque-producing device, and this torque is generated by the interaction of magnetic fields. The driving force is proportional to current and to the number of turns in the winding. This is often referred to as the amp-turns product. Essentially, the drive must act as a source of current. The stepping controller translates the step and direction signals into control waveforms for the driver. The step and direction signals are generated by clock-to-angle translation unit which is tied to host computer through USB interface. The USB interface used poses the high speed general purpose parallel interface (GPIF). Communication bridge is needed to connect the stepping control units and the GPIF.

The other most important unit is the radiometry part. It consists of the sensor and sensor controller, responsible for sensor conditioning, power supply. As the sensed light radiation level is converted to frequency at sensor output, frequency meter is needed to measure the obtained value. Reference oscillator is a quartz crystal with oscillation schematic and frequency multiplier. The radiometry section control is also accomplished via host computer, communication via USB interface is using GPIF bridge.

LED is controlled by current source. LED current control circuit stability over time and temperature is quite important since the  $I_v$  fluctuation even within same manufacturing lot is quite significant (refer to [7]). The current output DAC AD420 has been used as the current source. The AD420 is a complete digital to current loop output converter, designed to meet the needs of the industrial control market. It provides a high precision, fully integrated, low cost single-chip solution for generating current loop signals. The output current range is (0-24) mA. This DAC uses sigma-delta ( $\Sigma\Delta$ ) DAC technology to achieve a 16-bit resolution. Since LED optical performance is temperature dependant [7] there is a significant fluctuation over time at the initial moment (cold start). The useful indicator for stabilization of the  $I_v$  can be the LED forward bias voltage  $V_f$  - it is fluctuating in correlation to  $I_v$ . Therefore a digital voltmeter has been added for  $V_f$  monitoring. Both the current source and the voltmeter are controlled via the host computer via USB interface. The GPIF bridge is used for connection to USB.

All the communication with the host computer are accomplished using the Cypress Semiconductor Corporation's EZ-USB FX2LP IC CY7C68013A. It is a highly integrated, low-power USB2.0 microcontroller. The USB2.0 transceiver, serial interface engine (SIE), enhanced 8051 microcontroller and a programmable peripheral interface are integrated in a single chip. The FX2LP architecture results in data transfer rates of over 53 Mbytes per second, the maximum-allowable USB 2.0 bandwidth, while still using an integrated low-cost 8051 microcontroller. Cypress's smart SIE handles most of the USB protocol in hardware, freeing the embedded microcontroller for application-specific functions.

The uncertainties sources of measurements and estimation of the achievable accuracy have been analyzed in [7]. The LED half power angle  $2\Theta_{0.5}$  measurement expanded uncertainty was evaluated to be  $0.53^\circ$ . For reader convenience we only present the percentage of these uncertainties contribution in Fig. 8.

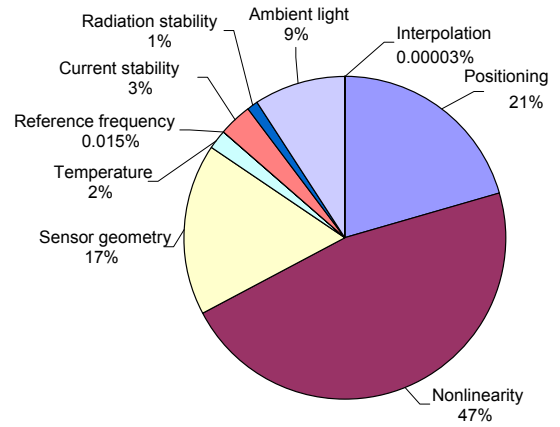


Fig. 8. Uncertainty sources for angle  $2\Theta_{0.5}$  measurement

Graph in Fig. 8 indicate that  $2\Theta_{0.5}$  measurement uncertainty caused by sensor nonlinearity is prevailing here. Let's investigate the uncertainty term caused by sensor nonlinearity. According to [7],  $I_v$  angular distribution for point sources with rotational symmetry and various viewing angles can be approximated as:

$$I_v(\Theta) = I_{v\max} \cos(\Theta)^{g-1}, \quad (4)$$

where  $I_{v\max}$  is LED peak luminous intensity at angle normal to the source itself and  $g$  is a coefficient, proportional to viewing angle.

Sensor nonlinearity usually is described as difference between the real line representing the sensor response and ideal straight line connecting the zero and full scale (F.S.) points. Readers can turn to [10] for more detailed explanation and error evaluation methods. We concentrate on worst case - when specified error is appearing at half power level in LED FFP. Assuming the derivative at this point is the sensitivity coefficient, solving (4) for  $\Theta$  one will get the angle measurement sensitivity for FFP:

$$\frac{d\theta}{dI_v} = \frac{1}{0.5^{g-1} \sqrt{1 - 0.5^{g-1}}}. \quad (5)$$

It can be scaled to be expressed in degrees per nonlinearity %, as plotted in Fig. 9.

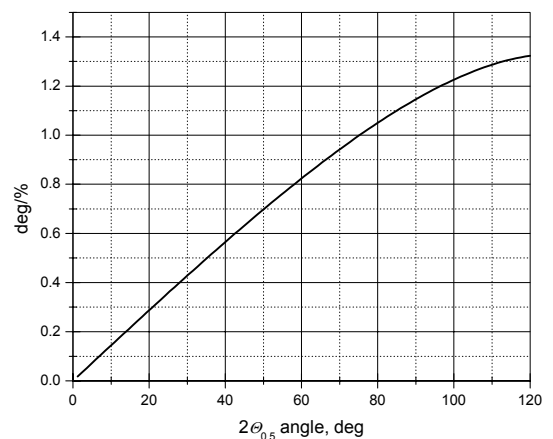


Fig. 9. Angle error for  $2\Theta_{0.5}$  versus sensor nonlinearity

The Fig. 9 graph indicates that sensor with smaller nonlinearity is needed in order to reduce the combined standard uncertainty. The Table 1 lists the new (as of used in [7]) set of candidate sensors.

**Table 1.** Radiometry sensors

Part	Area, mm <sup>2</sup>	Range, μW/cm <sup>2</sup>	Linearity, %
TCS230	1.4	0.01-500	0.5
TCS230	1.4	0.01-50	0.2
TCS230	1.4	0.01-5	0.1
TSL245	1	0.02-40	0.2
NT57523	5.2	0.182-64000	0.2
SED033	33	0.00015-154	0.1

The prototype system used the TCS230 sensor. Revising the candidate list and we still consider TCS230 as best candidate. Here is the reasoning - if LED distance to sensor is kept more than 170mm and LED brightness is below 10000mcd (professional LED for video screen will not be above 5000mcd) then middle radiation range condition is met. Sensor can be considered 0.2% linearity, reducing the nonlinearity – caused uncertainty term by more than three times (0.5% vs 0.2% and 1.2°% sensitivity for 110° LED from Fig.8). Also, it has a reasonable measurement range and the price is much lower than NT57523.

The LED peak emission direction  $\theta_{\text{peak}}$  angle expanded uncertainty was evaluated using a prototype system in [7] to be 0.39°. Again, skipping the data presented in the forementioned publication for the sake of simplicity we indicate only the percentage of the constituting uncertainties in Fig. 10.

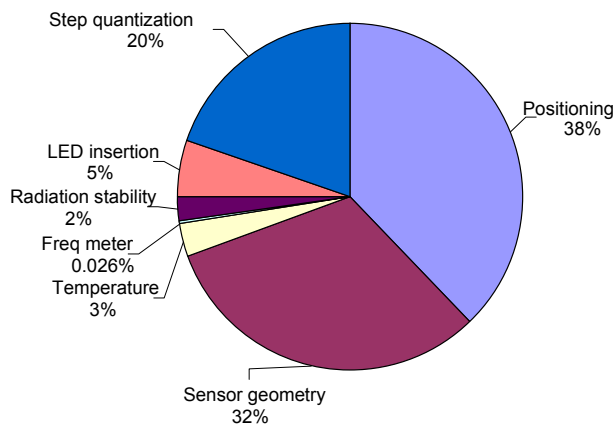


**Fig. 10.** Uncertainty sources for angle  $\theta_{\text{peak}}$  measurement

Here the prevailing error source is caused by the positioning errors (38%). This has been obtained by using the conventional step motor driver L6219 which has only triple microstepping possibility. Using the standard 1,8° step angle motor the 200 steps are obtained per revolution. By applying a micro stepping, angular resolution can be increased further. Using division by 4, 0.45° step is achieved, dividing by 6 - 0.3° step and so on. Typically a standard motor has a tolerance of +/- 5% non-accumulative error regarding the location of any given step [9]. This gives 2000 radial locations or 0.18°. Coincidentally this is

the resolution of a 10 microstep drive. Candidate microstepping motor drivers are listed in Table 2.

**Table 2.** Step motor drivers

Part	$I_{\text{max}}$ , A	$V_{\text{max}}$ , V	Microstepping, x
L6219	0.75	46	3
LB11946	1.2	50	4
TCA3727	0.75	50	3
SLA7060	1	46	16
LMD18245	3	55	4
R710	2	80	10
NJM37770	1.5	60	3
A3967	0.85	30	8

The SLA7060 driver seems the most attractive candidate, but as already been mentioned before standard step motor will not perform better than 10 step subdivision. R710 is an expensive driver intended for heavy duty industrial applications. Therefore, keeping in mind the driver used in prototype system had only 3 step subdivision we denominate the A3967 as the best candidate. Further increase of step subdivision will not allow reducing the combined uncertainty since the other sources will start prevailing (refer Fig. 10).

### Measurements results of LED directivity

The system was used for several manufacturers LED FFP measurement. The LEDs used for investigation are dedicated for large size LED video screens manufacturing, therefore exhibit wide viewing angle which has been specified by all manufacturers as 110°. LEDs are chosen on similar in order to eliminate the wavelength related differences in directivity. Since red LED technology is most mature, the best FFP accuracy is expected for this color LEDs. The LED dominant emission wavelength is chosen close to most popular in video screens - 623nm. Since manufacturer names and LED brands are not important here we use the abbreviated notation.

The LED FFP has been measured. Then several LED of the same manufacturer same manufacturing lot was averaged and resulting FFP normalized to peak emission value. Refer the Fig. 11 for diagrams of several LED and their averaged result (thick line). The normalized FFP was used in further investigation.

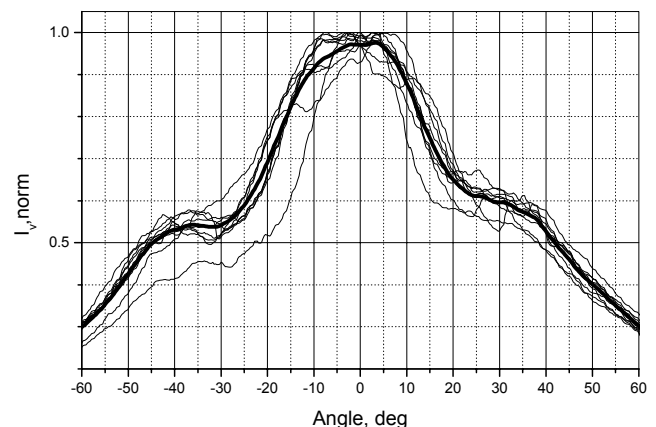


**Fig. 11.** Averaged normalized FFP for D10 LED

Instead of Cartesian coordinate system, screen FFP can be presented as polar diagram (refer Fig. 12).

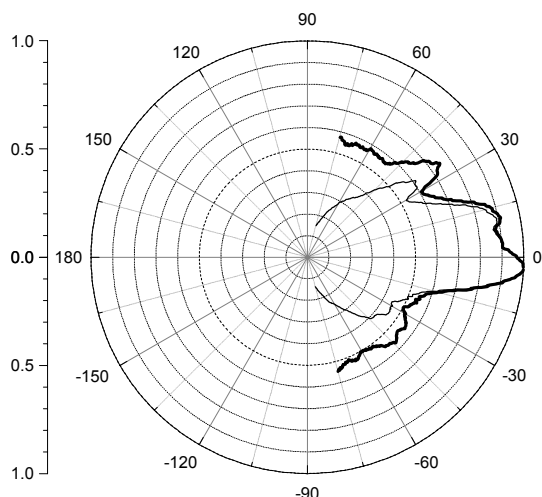


Fig. 12. Calculated D10 screen FFP in polar system

As planned, same averaging procedure has been performed on several manufacturers' diodes (Fig. 13).

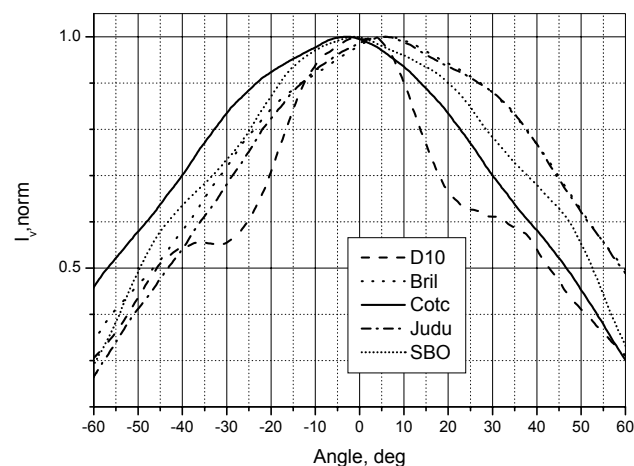


Fig. 13. Various manufacturers LED FFP

Now it would make sense to use the averaged LED FFP from multiple measurements for several manufacturers' diodes in order to construct the screen FFP (Fig. 14).

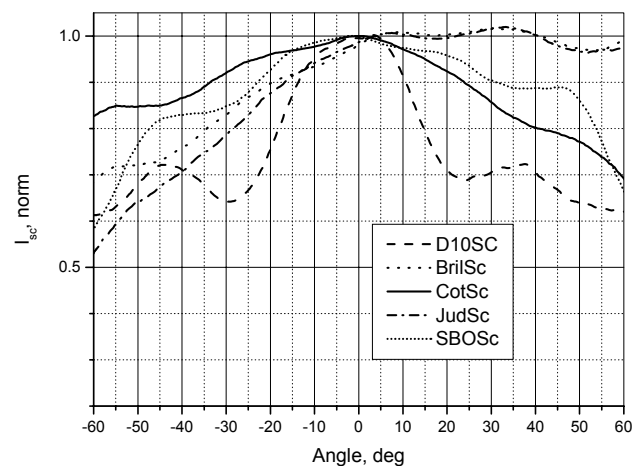


Fig. 14. Various manufacturers LED FFP

Multiple LED response will closer represent the resulting screen FFP. As it could be expected the flattest screen FFP has been obtained for Cotco LED LO5SMNHR4. This LED type (named "Screen Master") is exceptional because it is dedicated for professional LED video screens.

## Conclusions

In general, the result of a measurement is only an approximation or estimate of the value of the specific quantity subject to measurement. The goniometry system is developed for LED directivity investigation. The analysis of the new goniometry system measurement uncertainty sources and combined uncertainty evaluation still has to be done. Some measurement conditions are defined by CIE. The system developed does not exactly meet the recommended conditions. The reason is simple – the integrating spheres and the accompanying equipment are very expensive. But the system developed allows the professional LED video screen manufacturer to assess the level of incoming LEDs and to compare them between various manufacturers. And all is at a fraction of cost which would have been paid for professional LED goniometry system.

The various manufacturers LED FFP measurement results indicate that despite similar specified directivity parameters resulting screen FFP vary significantly so the appearance for the spectator.

## References

1. **Watanabe Nobuo.** Recent LED display devices // Japanese Railway Engineering. – 1992. – No. 119. – P. 6–8.
2. **Miyoshi Morimasa, Tsujikado Kazumi, Fukumura Shinji.** Large-scale color LED stock-information display board // National Technical Report (Matsushita Electric Industry Company). 1987. – Vol. 33, No 1. – P. 102–107.
3. **Abramov V.S., Puisha A.E., Polyakova I.P., Tomilin, M.G., Chuvashov, A.I.** LED modules for large screens // Journal of Optical Technology (Opticheskii Zhurnal). – 2003. – Vol.70, No.7. – P.492–494.
4. LED Metrology Handbook of LED Metrology Instrument Systems GmbH 2000. – P. 1–40.
5. The radiometry of Light Emitting Diodes. Technical guide. Labsphere Inc. UK. – 2001. – P. 1–18.
6. **Commission Internationale de l'Éclairage:** Measurement of LEDs, CIE 127-1997.
7. **Svilainis L., Dumbrava V.** LED goniometry: the feasibility study // Matavimai. – Kaunas: Technologija. – 2005 – Nr.3(35). – P. 35–40.
8. **Brett Wendler.** LED Viewing Angles vs. LED Video Display Viewing Angles Technical Note 40 Daktronics, Inc. – 2002. – P. 1.
9. **Hopkins T. L.** Stepper motor driver considerations: common problems and solutions. AN 460. SGS-Thompson electronics.USA. – 1992 – P. 1–12.
10. **Nyce, David S.** Linear Position Sensors: Theory and Application. John Wiley & Sons, Inc. – 2004. – P. 13.

**L. Svilainis, V. Dumbrava. LED Goniometry System // Electronics and Electrical Engineering. – Kaunas: Technologija, 2006 – No. 8(72). – P. 69–74.**

The light emitting diode (LED) directional parameters measurement system is analysed. It has been indicated that positioning uncertainty is the major contributing member in LED peak emission angle  $\theta_{\text{peak}}$  measurement. The LED half power emission angle  $\theta_{0.5}$  combined uncertainty is mainly contributed by radiometry sensor nonlinearity. New measurement system has been developed basing the prototype system. The new computer – controlled system design approach is described. System capabilities are demonstrated by far-field-pattern (FFP) measurement results of various manufacturers LEDs. The measured LED FFP are recalculated into totaling whole screen directivity diagrams using the averaged LED FFP from multiple measurements. The diagrams are presented both in Cartesian and polar coordinate system. Ill.14, bibl.10 (in English; summaries in English, Russian and Lithuanian).

**Л. Свилайнис, В. Думбрава. Система для измерения параметров свето-излучающих диодов // Электроника и электротехника. – Каунас: Технология, 2006. – № 8(72). – С. 69–74.**

Исследуются вопросы связаны с измерением диаграмм направленности для свето-излучающих диодов. Показано, что при измерении максимального угла излучения света  $\theta_{\text{peak}}$  наибольшее влияние на суммарную неопределенность результата измерения имеет погрешность устройства позиционирования диодов. При измерении угла половины мощности излучения  $\theta_{0.5}$ , наибольшее влияние на суммарную неопределенность результата измерения имеет погрешность нелинейности светового сенсора. Создана и описана новая компьютерная система для измерения диаграмм направленности светоизлучающих диодов на основе прототипной системы. Экспериментально измерены и приведены графики диаграмм направленности свето излучающих диодов и свето излучающих экранов для разных изготовителей в Декартовой или в полюсной системе отображения. Ил.14, библи.10. (на английском языке; рефераты на английском, русском и литовском яз.).

**L. Svilainis, V. Dumbrava. Goniometrinė šviesos diodų matavimo sistema // Elektronika ir elektrotechnika. – Kaunas: Technologija, 2006 – Nr. 8(72). – P. 69–74.**

Nagrinėjama šviesos diodų kryptingumo parametrų matavimo sistema. Parodyta, kad matuojant šviesos diodų maksimalų spinduliavimo kampą  $\theta_{\text{peak}}$ , didžiausią įtaką matavimų rezultatų suminei neapibrėžčiai turi diodo pozicionavimo sando narys. Matuojant šviesos diodų pusės galios spinduliavimo kampą  $\theta_{0.5}$ , didžiausią įtaką suminei neapibrėžčiai turi šviesos jutiklio netiesiškumo sandas. Remiantis prototipine šviesos diodų matavimo sistema, sukurta ir aprašyta nauja kompiuterinė šviesos diodų kampinių parametrų matavimo sistema. Darbe pateiktos konkrečių šviesos diodų gamintojų kryptingumo diagramos Dekarto ar polinėje koordinačių sistemoje, tiek pavienių diodų, tiek perskaičiuotų švieslentėms polinėje koordinačių sistemoje. Il.14, bibl.10. (anglų kalba; santraukos anglų, rusų ir lietuvių k.).